

# Substrate and Solvent Influence on the Photochemical C–H Bond Activation Reactivity of (HBPz'<sub>3</sub>)Rh(CO)<sub>2</sub> (Pz' = 3,5-Dimethylpyrazolyl)

Agus A. Purwoko, Stephen D. Tibensky, and Alistair J. Lees\*

Department of Chemistry, State University of New York at Binghamton,  
Binghamton, New York 13902-6016

Received May 1, 1996<sup>⊗</sup>

The photochemically-induced intermolecular C–H bond activation reaction of (HBPz'<sub>3</sub>)Rh(CO)<sub>2</sub> (Pz' = 3,5-dimethylpyrazolyl) has been investigated in various hydrocarbon solutions at 293 K following excitation at 366 and 458 nm. UV–visible and FTIR spectra recorded throughout photolysis illustrate that the dicarbonyl complex can be converted readily to the corresponding (HBPz'<sub>3</sub>)Rh(CO)(R)H derivatives at each of the excitation wavelengths. The photochemistry proceeds without interference from secondary photoprocesses or thermal reactions and the reactivity has been measured quantitatively with the determination of absolute quantum efficiencies for intermolecular C–H bond activation ( $\phi_{\text{CH}}$ ). These measurements indicate that the C–H activation reaction proceeds very efficiently ( $\phi_{\text{CH}} = 0.13\text{--}0.32$ ) on excitation at 366 nm but is much less effective ( $\phi_{\text{CH}} = 0.0059\text{--}0.011$ ) on photolysis at 458 nm for each of the hydrocarbon substrates. The observed dependence of  $\phi_{\text{CH}}$  on irradiation wavelength is consistent with different reactivities from two rapidly dissociating low-energy ligand field (LF) excited states and the generation of monocarbonyl (HBPz'<sub>3</sub>)Rh(CO) and ligand-dechelated ( $\eta^2$ -HBPz'<sub>3</sub>)Rh(CO)<sub>2</sub> intermediates upon UV and visible excitation, respectively. The former species is attributed to be responsible for the unusually efficient C–H bond activation, whereas it is suggested that the latter complex effectively lowers the quantum efficiency by undergoing a facile  $\eta^2 \rightarrow \eta^3$  ligand rechelation process. Significantly, the photoefficiencies are found to be unaffected on increasing the dissolved CO concentration, illustrating that the monocarbonyl reaction intermediate is extremely short-lived and is solvated before CO is able to coordinate. Additionally, the lack of a [CO] dependence on  $\phi_{\text{CH}}$  indicates that this solvated intermediate is not subject to a competitive back-reaction with CO prior to the C–H activation step, illustrating that the quantum efficiencies in (HBPz'<sub>3</sub>)Rh(CO)<sub>2</sub> appear to be solely determined by the branching ratio between the dissociative and nondissociative routes. At any particular excitation wavelength the photoefficiencies are observed to be similar across the series of alkanes but are significantly reduced for the aromatic solvents, even though the aryl hydrido photoproducts are found to be more thermodynamically stable. These  $\phi_{\text{CH}}$  differences are also rationalized in terms of photophysical effects on the upper LF level and are related to variations in the nonradiative relaxation rates for the excited (HBPz'<sub>3</sub>)Rh(CO)<sub>2</sub> complex in the hydrocarbon solutions.

## Introduction

Considerable attention has been paid in recent years to the photochemistry of transition-metal organometallic complexes that facilitate C–H bond activation of hydrocarbon substrates.<sup>1</sup> The CpM(CO)<sub>2</sub> and Cp\*M(CO)<sub>2</sub> (Cp =  $\eta^5$ -C<sub>5</sub>H<sub>5</sub>; Cp\* =  $\eta^5$ -C<sub>5</sub>Me<sub>5</sub>; M = Rh, Ir) complexes have been of particular interest since the initial discovery of their light-induced intermolecular C–H activation processes.<sup>2</sup> Following extensive study of these and related systems, much has been learned about the identity and reactivity of the photochemical intermediates in such oxidative addition reactions. For instance, in the CpRhL<sub>2</sub> and Cp\*RhL<sub>2</sub> (L = CO, PR<sub>3</sub>, C<sub>2</sub>H<sub>4</sub>) systems it has been clearly shown that the C–H activation mechanism involves the initial formation of CpRhL and Cp\*RhL primary photoproducts. These species are solvated extremely rapidly in even normally

inert solvents prior to reacting with the R–H bond. Results obtained from spectroscopic studies in liquefied noble gas solvents,<sup>3</sup> matrix isolation spectroscopy,<sup>4</sup> laser-flash photolysis,<sup>5</sup> steady-state photolysis<sup>6</sup> and theoretical calculations<sup>7</sup> are all in accordance with the initial formation of a highly reactive 16-electron intermediate. The photoreactions are known to take

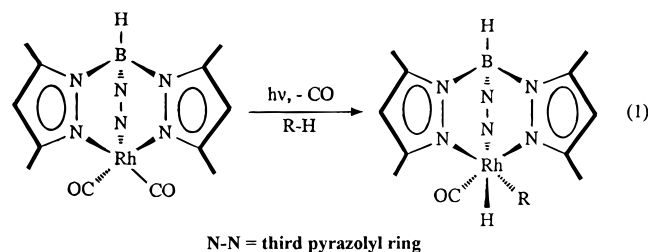
<sup>⊗</sup> Abstract published in *Advance ACS Abstracts*, November 1, 1996.

- (1) (a) Perutz, R. N. *Chem. Soc. Rev.* **1993**, 361. (b) Crabtree, R. H. *The Organometallic Chemistry of the Transition Metals*, 2nd ed.; Wiley-Interscience: New York, 1994; p 321. (c) Arndtsen, B. A.; Bergman, R. G.; Mobley, T. A.; Peterson, T. H. *Acc. Chem. Res.* **1995**, 28, 154.
- (2) (a) Janowicz, A. H.; Bergman, R. G. *J. Am. Chem. Soc.* **1982**, (b) Janowicz, A. H.; Bergman, R. G. *J. Am. Chem. Soc.* **104**, 352. (c) Janowicz, A. H.; Bergman, R. G. *J. Am. Chem. Soc.* **1983**, **105**, 3929. (d) Hoyano, J. K.; Graham, W. A. G. *J. Am. Chem. Soc.* **1982**, **104**, 3723. (e) Hoyano, J. K.; McMaster, A. D.; Graham, W. A. G. *J. Am. Chem. Soc.* **1983**, **105**, 7190.

- (3) (a) Haddleton, D. M.; Perutz, R. N.; Jackson, S. A.; Upmacis, R. K.; Poliakoff, M. *J. Organomet. Chem.* **1986**, **311**, C15. (b) Sponsler, M. B.; Weiller, B. H.; Stoutland, P. O.; Bergman, R. G. *J. Am. Chem. Soc.* **1989**, **111**, 6841. (c) Weiller, B. H.; Wasserman, E. P.; Bergman, R. G.; Moore, C. B.; Pimentel, G. C. *J. Am. Chem. Soc.* **1989**, **111**, 8288. (d) Weiller, B. H.; Wasserman, E. P.; Moore, C. B.; Bergman, R. G.; *J. Am. Chem. Soc.* **1993**, **115**, 4326.
- (4) (a) Rest, A. J.; Whitwell, I.; Graham, W. A. G.; Hoyano, J. K.; McMaster, A. D. *J. Chem. Soc., Chem. Commun.* **1984**, 624. (b) Haddleton, D. M.; Perutz, R. N. *J. Chem. Soc., Chem. Commun.* **1985**, 1372. (c) Bloyce, P. E.; Rest, A. J.; Whitwell, I.; Graham, W. A. G.; Holmes-Smith, R. *J. Chem. Soc., Chem. Commun.* **1988**, 846. (d) Rest, A. J.; Whitwell, I.; Graham, W. A. G.; Hoyano, J. K.; McMaster, A. D. *J. Chem. Soc., Dalton Trans.* **1987**, 1181. (e) Haddleton, D. M.; McCramley, A.; Perutz, R. N. *J. Am. Chem. Soc.* **1988**, **110**, 1810.
- (5) (a) Belt, S. T.; Haddleton, D. M.; Perutz, R. N.; Smith, B. P. H.; Dixon, A. J. *J. Chem. Soc., Chem. Commun.* **1987**, 1347. (b) Belt, S. T.; Grevels, F.-W.; Koltzbücher, W. E.; McCamley, A.; Perutz, R. N. *J. Am. Chem. Soc.* **1989**, **111**, 8373.
- (6) (a) Drolet, D. P.; Lees, A. J. *J. Am. Chem. Soc.* **1990**, **112**, 5878. (b) Drolet, D. P.; Lees, A. J. *J. Am. Chem. Soc.* **1992**, **114**, 4186. (c) Purwoko, A. A.; Lees, A. J. *Coord. Chem. Rev.* **1994**, **132**, 155. (d) Purwoko, A. A.; Drolet, D. P.; Lees, A. J. *Organomet. Chem.* **1995**, **504**, 107.

place on a picosecond time scale<sup>8</sup> and are understood to arise from rapidly dissociating ligand field excited states.<sup>6</sup> Recently, the rates of oxidative addition of both CpRh(CO)<sub>2</sub> and Cp\*Rh(CO)X (X = Kr, Xe) with alkanes have been determined in the gas phase and in liquefied rare gas solutions, respectively.<sup>9</sup>

The related (HBPz'<sub>3</sub>)Rh(CO)<sub>2</sub> (Pz' = 3,5-dimethylpyrazolyl) complex is clearly another C–H activating system of considerable importance, having been shown to undergo oxidative addition readily with both saturated and unsaturated hydrocarbons following visible light exposure at room temperature (see eq 1).<sup>10</sup> Consequently, we recently embarked on an investigation



of the solution photochemistry of (HBPz'<sub>3</sub>)Rh(CO)<sub>2</sub> and in the course of this work have measured absolute quantum efficiencies for the C–H activation process ( $\phi_{CH}$ ) in various alkanes.<sup>11</sup> Importantly, the photochemical reaction of the (HBPz'<sub>3</sub>)Rh(CO)<sub>2</sub> complex to form the hydrido photoproduct has been determined to be unusually clean and very efficient ( $\phi_{CH} = 0.31$ – $0.32$  at 366 nm) in alkanes at room temperature. The photochemical conversion was, in fact, found to proceed completely without any interference from either secondary photoprocesses or thermal reactions, making it feasible to measure the  $\phi_{CH}$  values directly from spectroscopic data of the intermolecular C–H bond activation reaction in room-temperature solution. In contrast, the C–H activation quantum efficiencies for the CpRh(CO)<sub>2</sub> and Cp\*Rh(CO)<sub>2</sub> systems have had to be derived from photochemical ligand substitution and Si–H bond activation results.<sup>6</sup>

Although a number of the key steps in the oxidative addition chemistry of these cyclopentadienyl- and (tris(pyrazolyl)borato)-rhodium dicarbonyl complexes are now known, much remains to be understood about the role of the hydrocarbon substrate in these solution reactions. As noted above, the (HBPz'<sub>3</sub>)Rh(CO)<sub>2</sub> complex provides the opportunity to spectroscopically measure the photochemical reactivity directly, and therefore we have studied the photochemistry of this complex in a variety of hydrocarbon solvents. Here we report the results of our investigation of photoreactivity for a series of RH substrates, including quantitative determinations of the photochemistry following excitation at different wavelengths.

## Experimental Section

**Materials.** Potassium hydrotris(3,5-dimethylpyrazol-1-yl)borate and 3,5-dimethylpyrazole were purchased from Aldrich Chemical Co. in high purity (97%) and used as received. Chlorodicarbonylrhodium(I) dimer was obtained in high purity (>99%) from Strem Chemicals, Inc. and used without further purification. Solvents and reagents used in the preparation of (HBPz'<sub>3</sub>)Rh(CO)<sub>2</sub> were obtained and purified as previously described.<sup>11b</sup> Solvents used in the photoreactivity measurements were purchased from Fisher Scientific Co. and Aldrich Chemical Co. as spectroscopic grade. Nitrogen gas used for solvent deoxygenation was purchased as high research grade (Union Carbide, >99.99% purity) and was itself deoxygenated and dried by passage over calcium sulfate (W. A. Hammond Co.), phosphorus pentoxide (Aldrich Chemical Co.), and a pelletized copper catalyst (BASF R3-11, Chemical Dynamics Co.) that had been activated with hydrogen gas (Union Carbide, >99% purity), according to a previously described procedure.<sup>12</sup> Carbon monoxide (Union Carbide, 99.5% purity) used in the photoreactivity studies was further purified by passage through a 1-m tube (2-cm diameter) containing the above copper catalyst and then a 25-cm tube (4-cm diameter) containing a mixture of calcium sulfate and 5-Å molecular sieves.

**Synthesis.** The (HBPz'<sub>3</sub>)Rh(CO)<sub>2</sub> complex was prepared via reaction of chlorodicarbonylrhodium(I) dimer with potassium hydrotris(3,5-dimethylpyrazolyl)borate according to a previously described procedure.<sup>10b</sup> A suspension of K[HBPz'<sub>3</sub>] (2.38 mmol) was formed by stirring in toluene (70 mL) for 15 min and [Rh(CO)<sub>2</sub>Cl]<sub>2</sub> (1.03 mmol) was subsequently added. This reaction mixture was stirred in the dark for 2.5 h at room temperature and then filtered to remove KCl and any other unreacted materials. Subsequently, the filtrate was cooled to  $-20$  °C for 24 h to form an orange-yellow solid which was dried *in vacuo*. The supernatant fluid was concentrated to approximately one half the original volume and cooled to  $-20$  °C for a further 48 h, yielding additional solid product. IR for (HBPz'<sub>3</sub>)Rh(CO)<sub>2</sub> in *n*-pentane:  $\nu(\text{CO})$  2054, 1980  $\text{cm}^{-1}$  (lit.<sup>10a</sup> in *n*-hexane:  $\nu(\text{CO})$  2054, 1981  $\text{cm}^{-1}$ ). UV-visible for (HBPz'<sub>3</sub>)Rh(CO)<sub>2</sub> in *n*-pentane:  $\lambda_{\text{max}} = 356$  nm,  $\epsilon = 2100$   $\text{M}^{-1} \text{cm}^{-1}$  (lit.<sup>10a</sup> in *n*-hexane:  $\lambda_{\text{max}} = 353$  nm,  $\epsilon = 1820$   $\text{M}^{-1} \text{cm}^{-1}$ ). Mp = 205 °C dec.

**Photochemical Procedures.** UV photolyses at 366 nm were performed with light from an Ealing Corp. medium-pressure 200-W mercury arc lamp and housing apparatus set on an optical rail. A bandpass interference filter (10 nm, Ealing Corp.) was used to isolate the excitation wavelength, and a solvent filter was placed between the sample and the lamp to ensure that IR from the light source did not heat up the solution. The incident light intensities were determined by ferrioxalate<sup>13</sup> and Aberchrome 540 actinometry,<sup>14</sup> and were typically in the range of  $5.2 \times 10^{-7}$  to  $1.1 \times 10^{-6}$  einstein  $\text{min}^{-1}$ . Visible excitations at 458 nm were carried out with a Lexel Corp. Model 95-4 4 W argon-ion laser; the incident laser light intensity was calibrated by means of a Lexel Corp. Model 504 external power meter. Typically, laser powers of 30–60 mW ( $6.9 \times 10^{-6}$  to  $1.4 \times 10^{-5}$  einstein  $\text{min}^{-1}$ ) were employed for these 458-nm irradiations, although results were also obtained with reduced laser light powers of between 10 and 20 mW and the measured quantum efficiency values were unchanged.

During these irradiation experiments the solution temperatures were controlled to  $\pm 0.1$  K by circulating a thermostated ethylene glycol–water mixture through a jacketed cell holder. Prior to light excitation, the solutions were stringently filtered through 0.22- $\mu\text{m}$  Millipore filters and deoxygenated by purging with prepurified nitrogen gas for 15 min. Throughout photolysis the solutions were rapidly stirred to ensure sample homogeneity and a uniform absorbance in the light path. Solutions saturated with CO were prepared by initially bubbling CO gas through the solution for 30 min and subsequently stirring the solution for a further 30 min under a sealed CO atmosphere. UV-visible and FTIR spectra were obtained from solutions at regular intervals throughout irradiation; resultant quantum efficiency results were determined in triplicate and were found to be reproducible to

- (7) (a) Saillard, J.-Y.; Hoffman, R. *J. Am. Chem. Soc.* **1984**, *106*, 2006. (b) Ziegler, T.; Tschinke, V.; Fan, L.; Becke, A. D. *J. Am. Chem. Soc.* **1989**, *111*, 9177.
- (8) (a) Dougherty, T. P.; Heilweil, E. J. *J. Chem. Phys.* **1994**, *100*, 4006. (b) Grubbs, W. T.; Dougherty, T. P.; Heilweil, E. J. *J. Chem. Phys. Lett.* **1994**, *227*, 480. (c) Dougherty, T. P.; Grubbs, W. T.; Heilweil, E. J. *J. Phys. Chem.* **1994**, *98*, 9396.
- (9) (a) Wasserman, E. P.; Moore, C. B.; Bergman, R. G. *Science* **1992**, *255*, 315. (b) Schultz, R. H.; Bengali, A. A.; Tauber, M. J.; Weiller, B. H.; Wasserman, E. P.; Kyle, K. R.; Moore, C. B.; Bergman, R. G. *J. Am. Chem. Soc.* **1994**, *116*, 7369. (c) Bengali, A. A.; Schultz, R. H.; Moore, C. B.; Bergman, R. G. *J. Am. Chem. Soc.* **1994**, *116*, 9585.
- (10) (a) Ghosh, C. K.; Graham, W. A. G. *J. Am. Chem. Soc.* **1987**, *109*, 4726. (b) Ghosh, C. K. Ph.D. Dissertation, University of Alberta, Edmonton, Alberta, Canada, 1988. (c) Bloyce, P. E.; Mascetti, J.; Rest, A. J. *J. Organomet. Chem.* **1993**, *444*, 223.
- (11) (a) Purwoko, A. A.; Lees, A. J. *Inorg. Chem.* **1995**, *34*, 424. (b) Purwoko, A. A.; Lees, A. J. *Inorg. Chem.* **1996**, *35*, 675.

- (12) Schadt, M. J.; Gresalfi, N. J.; Lees, A. J. *Inorg. Chem.* **1985**, *24*, 2492.
- (13) (a) Parker, C. A. *Proc. R. Soc. London, A* **1953**, *220*, 104. (b) Hatchard, C. G.; Parker, C. A. *Proc. R. Soc. London, A* **1956**, *235*, 518. (c) Calvert, J. G.; Pitts, J. N. *Photochemistry*; Wiley: New York, 1966.
- (14) Heller, H. G.; Langan, J. N. *J. Chem. Soc., Perkin Trans.* **1981**, 341.

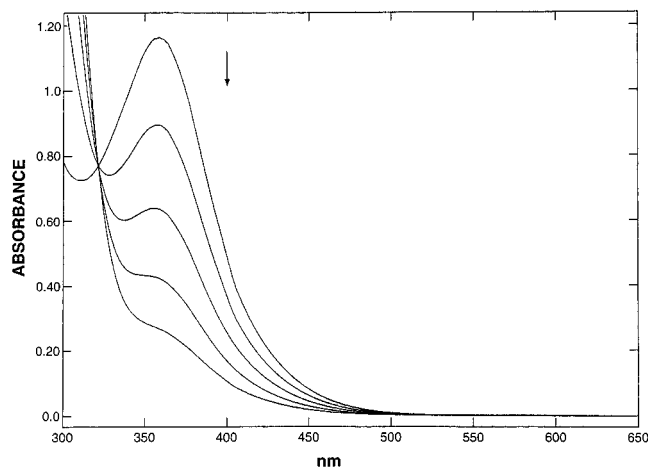


**Figure 1.** UV–visible absorption changes accompanying the 366-nm photolysis of  $(\text{HBPz}'_3)\text{Rh}(\text{CO})_2$  in deoxygenated mesitylene at 293 K. Spectra are depicted following 2-min irradiation time intervals; the initial spectrum was recorded prior to irradiation.

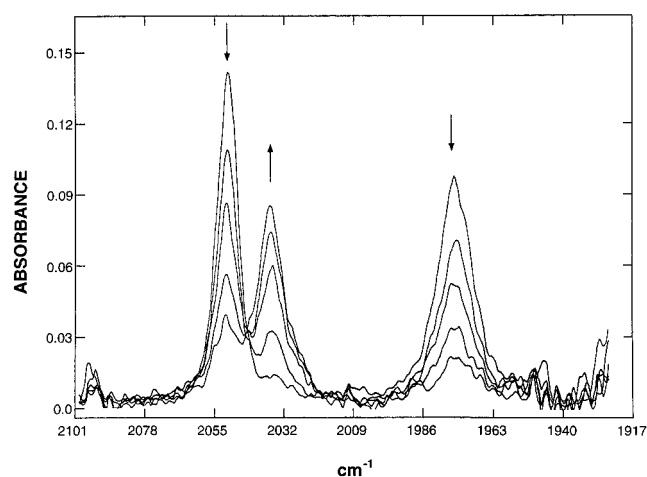


**Figure 2.** Infrared absorption changes accompanying the 366-nm photolysis of  $(\text{HBPz}'_3)\text{Rh}(\text{CO})_2$  in deoxygenated mesitylene at 293 K. Spectra are depicted following 2-min irradiation time intervals; the initial spectrum was recorded prior to irradiation.

within  $\pm 8\%$  from the mean value in each case. The C–H bond activation reactions were also measured in the dark to assess the extent of thermal processes and these were determined to be negligible during the course of the photolysis experiments.

UV–visible absorption spectra were obtained on a Hewlett-Packard Model 8450A diode-array spectrometer and the reported band maxima are considered accurate to  $\pm 2$  nm. Infrared spectra were recorded on a Nicolet Model 20SXC Fourier transform infrared (FTIR) spectrometer, and the reported band maxima are considered accurate to  $\pm 0.5$   $\text{cm}^{-1}$ . The infrared spectra were typically obtained from solutions using a NaCl cell of 1-mm path length.

## Results and Discussion

Photochemical excitations of  $(\text{HBPz}'_3)\text{Rh}(\text{CO})_2$  at wavelengths between 366 and 458 nm were performed in various deoxygenated hydrocarbon solutions at 293 K. Figure 1 depicts the UV–visible absorption spectra observed accompanying the 366-nm photolysis of the parent dicarbonyl complex in mesitylene at room temperature. During the reaction the lowest lying absorption band, centered at 359 nm, undergoes a substantial decline in intensity. Figure 2 shows the FTIR absorption spectral sequence recorded from the same irradiation experiment, illustrating the photochemical conversion of the dicarbonyl ( $\nu(\text{CO})$  at 2050 and 1975  $\text{cm}^{-1}$ ) to the monocarbonyl hydrido product ( $\nu(\text{CO})$  at 2036  $\text{cm}^{-1}$ ). These UV–visible and FTIR

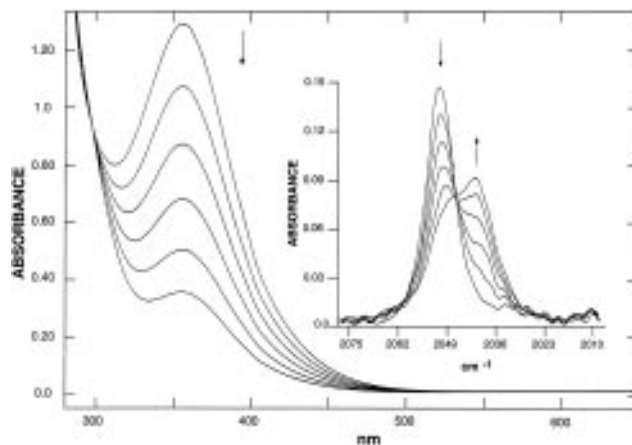


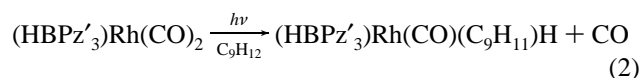
**Figure 3.** UV–visible and infrared (inset) changes accompanying the 366-nm photolysis of  $(\text{HBPz}'_3)\text{Rh}(\text{CO})_2$  in deoxygenated benzene at 293 K. Spectra are depicted following 2-min irradiation time intervals; the initial spectra recorded prior to irradiation.

**Table 1.** Infrared Carbonyl Stretching Bands for the Parent  $(\text{HBPz}'_3)\text{Rh}(\text{CO})_2$  complex and the  $(\text{HBPz}'_3)\text{Rh}(\text{CO})(\text{R})\text{H}$  Photoproducts in Solution at 293 K<sup>a</sup>

complex	solvent	$\nu(\text{CO}), \text{cm}^{-1}$
$(\text{HBPz}'_3)\text{Rh}(\text{CO})_2$	mesitylene	2050, 1975
$(\text{HBPz}'_3)\text{Rh}(\text{CO})(\text{C}_6\text{H}_5)\text{H}$	benzene	2045
$(\text{HBPz}'_3)\text{Rh}(\text{CO})(\text{C}_7\text{H}_7)\text{H}$	toluene	2042
$(\text{HBPz}'_3)\text{Rh}(\text{CO})(\text{C}_8\text{H}_9)\text{H}$	<i>p</i> -xylene	2040
$(\text{HBPz}'_3)\text{Rh}(\text{CO})(\text{C}_9\text{H}_{11})\text{H}$	mesitylene	2036
$(\text{HBPz}'_3)\text{Rh}(\text{CO})(\text{C}_5\text{H}_{11})\text{H}$	<i>n</i> -pentane	2029
$(\text{HBPz}'_3)\text{Rh}(\text{CO})(\text{C}_6\text{H}_{13})\text{H}$	<i>n</i> -hexane	2029
$(\text{HBPz}'_3)\text{Rh}(\text{CO})(\text{C}_7\text{H}_{15})\text{H}$	<i>n</i> -heptane	2028
$(\text{HBPz}'_3)\text{Rh}(\text{CO})(\text{C}_8\text{H}_{17})\text{H}$	isooctane	2028

<sup>a</sup> Alkane values were taken from ref 11b.

spectral changes are in complete agreement with the intermolecular C–H bond activation reaction (eq 2) initially described by Ghosh and Graham<sup>10a,b</sup> and the previously reported photochemical observations in alkane solutions.<sup>6d,11</sup>



Both UV–visible and FTIR spectra were recorded throughout the photolysis of  $(\text{HBPz}'_3)\text{Rh}(\text{CO})_2$  in all of the hydrocarbon solutions studied. Results obtained during the irradiation of the dicarbonyl complex in deoxygenated benzene are depicted in Figure 3. Again, the lowest energy UV–visible absorption band is observed to decrease in intensity, whereas the FTIR spectra reveal a sharp isosbestic point consistent with the smooth conversion of the dicarbonyl complex to form the hydrido photoproduct. In this latter sequence the lower energy  $\nu(\text{CO})$  band is masked by solvent absorption. These results are representative of those from the range of solvents studied; infrared data obtained from all of photochemical C–H bond activation reactions are summarized in Table 1.

The solution photochemistry observed here is apparently clean, and complete reaction conversions were achieved without significant interference from secondary photoprocesses or side reactions for each of the excitation wavelengths employed. Moreover, samples were monitored in the dark and reveal that there is a negligible amount of thermal reaction at 293 K taking place in the hydrocarbon solutions during the course of these photolysis experiments. The clean photochemical transformations of  $(\text{HBPz}'_3)\text{Rh}(\text{CO})_2$  have enabled us to quantitatively measure the photochemistry. Typically, data were acquired over reaction conversions of between 75 and 80%. Absolute

quantum efficiencies for intermolecular C–H bond activation ( $\phi_{\text{CH}}$ ) were determined by monitoring the decrease of the dicarbonyl's electronic absorption and infrared  $\nu(\text{CO})$  bands and application of eq 3. Here,  $C_{\text{R}}$  is the concentration of the reactant

$$-dC_{\text{R}}/dt = \phi_{\text{CH}}I_0(1 - 10^{-A_{\text{tot}}})\epsilon_{\text{R}}bC_{\text{R}}/A_{\text{tot}} \quad (3)$$

(HBPz'<sub>3</sub>)Rh(CO)<sub>2</sub> complex at varying photolysis times  $t$ ,  $I_0$  is the incident light intensity per unit solution volume,  $b$  is the cell pathlength, and  $A_{\text{tot}}$  and  $\epsilon_{\text{R}}$  are the absorbance of the solution and molar absorptivity of the reactant complex at the irradiation wavelength, respectively. The value  $A_{\text{tot}}$  is the total absorbance of the solution and represents both the parent and product species at the excitation wavelength; the component  $\epsilon_{\text{R}}bC_{\text{R}}/A_{\text{tot}}$  is the fraction of the absorbed light that is absorbed by the reactant complex in the solution mixture.<sup>15</sup> Thus, eq 3 accommodates the changing inner filter effects caused by the increasing light absorption of the photoproduct during the reaction, which is itself stable during the photolysis. Rearrangement and integration of eq 3 yields eqs 4–6,

$$d \ln C_{\text{R}} = -\phi_{\text{CH}}I_0\epsilon_{\text{R}}b[(1 - 10^{-A_{\text{tot}}})/A_{\text{tot}}] dt \quad (4)$$

$$\ln(C_i/C_o) = \alpha \int_{t_0}^{t_i} [(1 - 10^{-A_{\text{tot}}})/A_{\text{tot}}] dt \quad (5)$$

where

$$\alpha = -\phi_{\text{CH}}I_0\epsilon_{\text{R}}b \quad (6)$$

Plots of  $\ln[(A_t - A_{\infty})/(A_0 - A_{\infty})]$  vs  $\int_{t_0}^{t_i} [(1 - 10^{-A_{\text{tot}}})/A_{\text{tot}}] dt$ , where  $A_0$ ,  $A_t$ , and  $A_{\infty}$  are the infrared absorbance values of the reactant's  $\nu(\text{CO})$  bands during photolysis, were observed to yield straight lines of slope  $\alpha$  to reaction completion, with  $\alpha = -\phi_{\text{CH}}I_0\epsilon_{\text{R}}b$  (the value  $\alpha$  has units of reciprocal time). Coincident  $\alpha$  values are obtained following kinetic analysis at either of the reactant's  $\nu(\text{CO})$  bands. Moreover,  $\alpha$  values determined on monitoring the increasing  $\nu(\text{CO})$  absorbance of the hydrido photoproduct were identical for any particular experiment. These kinetic observations support the above conclusion that the photochemical conversion is uncomplicated by secondary processes. Additionally, the measured quantum efficiencies were in all cases found to be unaffected by variations in the incident light intensity (see Experimental Section), indicating that the solution was homogeneous and had, at any instance in time, a uniform absorbance throughout the light path in each of these photolyses.

Table 2 summarizes the determined absolute photochemical quantum efficiencies ( $\phi_{\text{CH}}$ ) for the intermolecular C–H bond activation reaction of (HBPz'<sub>3</sub>)Rh(CO)<sub>2</sub> in various hydrocarbon solutions at 293 K following both UV and visible excitations. In accordance with our previous results in alkanes, the  $\phi_{\text{CH}}$  data obtained from photolyses in all the hydrocarbon solvents are strongly dependent on the exciting wavelength.<sup>11b</sup> Clearly, the C–H activation pathway proceeds very effectively with excitation in the UV region (313, 366 nm), although this reaction is considerably less efficient following visible excitation (458 nm). These results lend further support to our earlier conclusion that there are two excited states with different reactivities in the (HBPz'<sub>3</sub>)Rh(CO)<sub>2</sub> system.<sup>6d,11</sup> Both electronically excited levels are attributed to be ligand field (LF) states, as the lowest absorption band is rather weak ( $\epsilon_{\text{max}} = 2100 \text{ M}^{-1} \text{ cm}^{-1}$  at 356 nm in *n*-pentane) and exhibits negligible solvent sensitivity. However, it is noticeable that this transition is substantially more

**Table 2.** Absolute Photochemical Quantum Efficiencies for the Intermolecular C–H Bond Activation Reaction of (HBPz'<sub>3</sub>)Rh(CO)<sub>2</sub> in Deoxygenated Hydrocarbon Solutions at 293 K<sup>a</sup>

solvent	$\lambda_{\text{ex}}$ , nm	$\phi_{\text{CH}}$
benzene	366	0.13
	458	0.0059
toluene	366	0.14
	458	0.0073
<i>p</i> -xylene	366	0.17
	458	0.0086
mesitylene	366	0.22
	458	0.0092
<i>n</i> -pentane	313	0.34
	366	0.32
	405	0.15
<i>n</i> -hexane	458	0.011
	366	0.31
	458	0.011
<i>n</i> -heptane	366	0.31
	458	0.010
	458	0.010
isooctane	366	0.31
	458	0.010

<sup>a</sup> Values were determined in triplicate and were reproducible to within  $\pm 8\%$ ; alkane data were taken from ref 11b.

intense than those of the corresponding CpM(CO)<sub>2</sub> and Cp\*M(CO)<sub>2</sub> (M = Rh, Ir) derivatives, implying possible contribution from a charge transfer component.<sup>6d</sup>

Excitation at 313 or 366 nm into the upper LF level occurs in a region that is recognized as being very effective for CO dissociation,<sup>17,18</sup> and an unsaturated monocarbonyl (HBPz'<sub>3</sub>)Rh(CO) complex is implicated to be the primary photoproduct at these short wavelengths. Moreover, in accordance with the extremely rapid radiationless and bond dissociation steps known to take place from the LF levels of metal carbonyl complexes,<sup>8,17,18</sup> it can be reasonably assumed that these events are completed within a few picoseconds and that the monocarbonyl complex is rapidly formed and solvated.<sup>11</sup> Indeed, preliminary femtosecond flash photolysis measurements recently performed on (HBPz'<sub>3</sub>)Rh(CO)<sub>2</sub> have illustrated that the primary photoproduct is a monocarbonyl fragment, which is produced and solvated within 10 ps.<sup>19</sup>

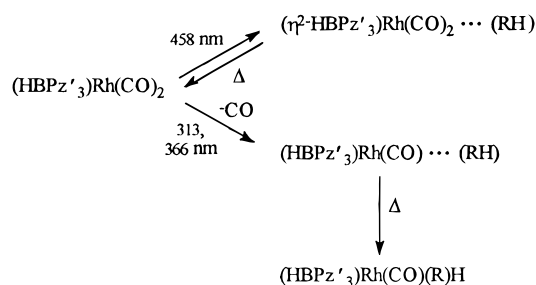
In comparison, excitation at 458 nm into the lower LF state yields ineffective C–H activation and the photochemistry can be explained by invoking a  $\eta^3 \rightarrow \eta^2$  ligand dechelation pathway. This route implicates an unsaturated ( $\eta^2$ -HBPz'<sub>3</sub>)Rh(CO)<sub>2</sub> intermediate which can also be expected to be rapidly solvated by the hydrocarbon molecules. The  $\eta^3 \leftrightarrow \eta^2$  ligand interconversion mechanism is already well-established in the thermal chemistry of (HBPz'<sub>3</sub>)Rh(CO)<sub>2</sub><sup>10b,11b</sup> and shown to be an extremely facile process. Such a pathway will serve to effectively lower the quantum efficiency because the ligand dechelation route is inconsequential with respect to the C–H activation chemistry; the initially photoproducted  $\eta^2$ -species

- (17) (a) Bonneau, R.; Kelly, J. M. *J. Am. Chem. Soc.* **1980**, *102*, 1220. (b) Lees, A. J.; Adamson, A. W. *Inorg. Chem.* **1981**, *20*, 4381. (c) Kelly, J. M.; Long, C.; Bonneau, R. *J. Phys. Chem.* **1983**, *87*, 3344. (d) Simon, J. D.; Xie, X. *J. Phys. Chem.* **1986**, *90*, 6751. (e) Simon, J. D.; Xie, X. *J. Phys. Chem.* **1987**, *91*, 5538. (f) Simon, J. D.; Xie, X. *J. Phys. Chem.* **1989**, *93*, 291. (g) Wang, L.; Zhu, X.; Spears, K. G. *J. Am. Chem. Soc.* **1988**, *110*, 8695.
- (18) (a) Joly, A. G.; Nelson, K. A. *J. Phys. Chem.* **1989**, *93*, 2876. (b) Lee, M.; Harris, C. B. *J. Am. Chem. Soc.* **1989**, *111*, 8963. (c) Xie, X.; Simon, J. D. *J. Am. Chem. Soc.* **1990**, *112*, 1130. (d) Yu, S.-C.; Xu, X.; Lingle, R.; Hopkins, J. B. *J. Am. Chem. Soc.* **1990**, *112*, 3668. (e) O'Driscoll, E.; Simon, J. D. *J. Am. Chem. Soc.* **1990**, *112*, 6580. (f) Dougherty, T. P.; Heilweil, E. J. *Chem. Phys. Lett.* **1994**, *227*, 19. (g) Arrivo, S. M.; Dougherty, T. P.; Grubbs, W. T.; Heilweil, E. J. *Chem. Phys. Lett.* **1995**, *235*, 247.
- (19) Lian, T.; Bromberg, S. E.; Yang, H.; Proulx, G.; Bergman, R. G.; Harris, C. B. *J. Am. Chem. Soc.* **1996**, *118*, 3769.

(15) Lees, A. J. *Anal. Chem.* **1996**, *68*, 226.

(16) Lawson, D. D. *Appl. Energy* **1980**, *6*, 241.

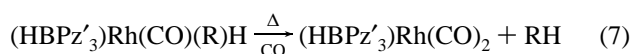
## Scheme 1



being simply returned to the parent dicarbonyl complex with no net photochemical conversion. Strictly speaking, though, the  $\phi_{\text{CH}}$  values at 458 nm ought to be zero for this reversible  $\eta^3 \rightarrow \eta^2$  photochemical mechanism, but the two LF bands are not resolved in the broad lowest-energy absorption envelope and the visible photolysis does not populate the lower LF state exclusively. Consequently, there is a small amount of C–H bond activation upon visible photolysis due to the partial population of the higher energy LF level. Scheme 1 summarizes the different reaction pathways implicated by the results.

It should be noted, however, that the  $\eta^3 \rightarrow \eta^2$  pathway is only one possible explanation for the wavelength dependence of  $\phi_{\text{CH}}$  and that spectroscopic identification of an  $(\eta^2\text{-HBPz}'_3)\text{Rh}(\text{CO})_2$  intermediate is necessary to confirm this mechanism. We are currently performing low-temperature experiments in liquid xenon in any effort to stabilize and identify any such species. It is appropriate, therefore, to consider alternative ways of rationalizing the quantum efficiency data. One possibility is that the lower energy level is unreactive but able to populate the higher energy state by thermal activation. However, previous studies of the temperature dependence of  $\phi_{\text{CH}}$  in *n*-pentane do not support this hypothesis as very low apparent activation energies of 8.3 ( $\pm 2.5$ ) and 5.4 ( $\pm 2.5$ ) kJ mol<sup>-1</sup> have been obtained following 366- and 458-nm photolysis, respectively.<sup>11b</sup> There is also the possibility that there is a third lower energy “dark” state which is completely unreactive and leads to ground state recovery, as concluded for several Co(III) complexes.<sup>20</sup> Finally, it may be that the photochemistry actually arises from a single excited state involving prompt and thermally-relaxed CO-dissociative pathways which give rise to different efficiencies.

Importantly, the photochemistry was also investigated when each of the solutions were prior saturated with CO gas and the addition of CO was not observed to influence the UV–visible and FTIR spectra or affect the  $\phi_{\text{CH}}$  data, at any of the exciting wavelengths. However, in the case of the alkane solvents, it was found that after CO bubbling of a photolyzed solution the parent complex was partially regenerated, according to eq 7, over a period of several hours at 293 K in the dark. This process was too slow to influence the measured quantum efficiencies. Significantly, no thermal regeneration of the starting complex was observed to take place for any of the aromatic solvents on bubbling with CO.



The lack of a [CO] dependence on  $\phi_{\text{CH}}$  strongly supports the conclusion that the primary photoproducts are formed extremely

rapidly from dissociative LF excited states and that the reaction intermediates are solvated before CO can coordinate. This kinetic observation is perhaps not surprising considering the concentration of dissolved CO in solution at 293 K (ca.  $7 \times 10^{-3}$  M in aromatic solvents and  $1 \times 10^{-2}$  M in alkanes)<sup>16</sup> compared to the concentrations of the hydrocarbon substrates (which range from 6.1 to 11.2 M). Importantly, though, the absence of any influence on  $\phi_{\text{CH}}$  with the addition of CO also indicates that the initially formed solvated monocarbonyl intermediate is not subject to a competitive thermal back-reaction with CO. In this connection, recent steady-state photolysis and ultrafast spectroscopic studies on CpRh(CO)<sub>2</sub> and Cp\*Rh(CO)<sub>2</sub> have also ruled out the possibility of either diffusional or geminate CO recombination processes affecting the quantum efficiencies.<sup>6b,21</sup>

On comparing the  $\phi_{\text{CH}}$  results for the different hydrocarbons in Table 2 it is significant to note that the quantum efficiency data for (HBPz'<sub>3</sub>)Rh(CO)<sub>2</sub> are similar at a common excitation wavelength for all the alkanes studied but are reduced for the aromatic solutions. This observation is somewhat surprising as the back-reaction with CO to form the parent complex is not a competitive process under these experimental conditions and so the differences in  $\phi_{\text{CH}}$  cannot be rationalized on the basis of varying kinetic reactivities of the substrate molecules. Moreover, the solvent viscosities for the various hydrocarbons are similar, and hence, there appears to be no evidence for solvent cage effects (and geminate CO recombination) influencing the  $\phi_{\text{CH}}$  values, as concluded for the CpRh(CO)<sub>2</sub> and Cp\*Rh(CO)<sub>2</sub> systems.<sup>6b,21</sup> Thus, the results clearly imply that the variations in  $\phi_{\text{CH}}$  are not brought about by solvent or substrate effects on the mechanism following the formation of the primary photo-product but are instead related to changes in the primary photophysical processes.

More specifically, it is the deactivation rates from the higher energy LF level (leading to the monocarbonyl species and responsible for C–H activation) which are being affected by the solvent medium. The data illustrate that in the case of the aromatic solvents the upper energy LF level appears to undergo more effective radiationless relaxation by nondissociative pathways. Notably, the degree of reduction in  $\phi_{\text{CH}}$  is observed to be similar for both the 366- and 458-nm photolyses; this is consistent with the above conclusion that the C–H activation photochemical mechanism derives from a single (upper LF) excited state. Apparently, as in the closely related cyclopentadienyl molecules,<sup>6b,21</sup> it is the branching ratio between the dissociative and nondissociative routes from this upper energy LF level that ultimately determines the photochemical efficiency. Furthermore, an even lower quantum efficiency at 366 nm of 0.11 at 293 K has been obtained from a photochemical kinetic study of (HBPz'<sub>3</sub>)Rh(CO)<sub>2</sub> decomposition in methanol. Overall, the  $\phi_{\text{CH}}$  results suggest that the solvent effects on the non-radiative decay rates from the complex are not simply related to solvent polarity but are perhaps analogous to the solvatochromic properties observed for other organometallic excited states.<sup>22</sup>

In an effort to make a comparison of the solvent data from (HBPz'<sub>3</sub>)Rh(CO)<sub>2</sub> to other systems, it is noticeable that there is a scarcity of studies reported in the literature on the photophysical properties of organometallic complexes under similar room temperature conditions to those studied here. Indeed, the investigation of luminescence from W(CO)<sub>5</sub>L [L = 4-acetyl-

(20) (a) Moggi, L.; Bolletta, F.; Balzani, V.; Scandola, F. *J. Inorg. Nucl. Chem.* **1966**, *28*, 2589. (b) Pribush, R. A.; Poon, C. K.; Bruce, C. M.; Adamson, A. W. *J. Am. Chem. Soc.* **1974**, *96*, 3027. (c) Wilson, R. B.; Solomon, E. I. *J. Am. Chem. Soc.* **1980**, *102*, 4085. (d) Langford, C. H. *Acc. Chem. Res.* **1984**, *17*, 96. (e) McCusker, J. K.; Walda, K. N.; Magde, D.; Hendrickson, D. N. *Inorg. Chem.* **1993**, *32*, 394.

(21) Bromberg, S. E.; Lian, T.; Bergman, R. G.; Harris, C. B. *J. Am. Chem. Soc.* **1996**, *118*, 2069.

(22) (a) Manuta, D. M.; Lees, A. J. *Inorg. Chem.* **1986**, *25*, 3212. (b) Lees, A. J. *Chem. Rev.* **1987**, *87*, 711.

**Table 3.** Luminescence Data<sup>a</sup> and Derived Photophysical Parameters for W(CO)<sub>5</sub>L Complexes in Deaerated Methylcyclohexane and Benzene at 298 K

complex	solvent							
	methylcyclohexane				benzene			
	10 <sup>4</sup> φ <sub>e</sub>	τ, ns	10 <sup>-3</sup> k <sub>r</sub> , s <sup>-1</sup>	10 <sup>-6</sup> k <sub>nr</sub> , s <sup>-1</sup>	10 <sup>4</sup> φ <sub>e</sub>	τ, ns	10 <sup>-3</sup> k <sub>r</sub> , s <sup>-1</sup>	10 <sup>-6</sup> k <sub>nr</sub> , s <sup>-1</sup>
W(CO) <sub>5</sub> (4-ACpy)	5.3	428	1.2	2.3	1.6	197	0.81	5.1
W(CO) <sub>5</sub> (4-BNpy)	7.7	459	1.7	2.2	2.3	190	1.2	5.3
W(CO) <sub>5</sub> (4-CNpy)	2.2	360	0.61	2.8	1.3	202	0.64	5.0

<sup>a</sup> Data were taken from ref 23.

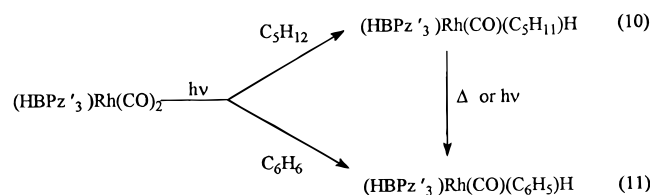
pyridine (4-ACpy), 4-benzoylpyridine (4-BNpy), 4-cyanopyridine (4-CNpy)] represents a rare case of an organometallic complex in which both the emission quantum efficiency (φ<sub>e</sub>) and emission lifetime (τ) have been measured in relevant nonpolar solutions at 298 K.<sup>23</sup> These results are shown in Table 3 and included are radiative (k<sub>r</sub>) and nonradiative (k<sub>nr</sub>) rate constants derived from the emission values by application of eqs 8 and 9. Clearly, the k<sub>nr</sub> values are most pertinent to the

$$k_r = \phi_e / \tau \quad (8)$$

$$k_{nr} = (1/\tau) - k_r \quad (9)$$

current system, as (HBPz'<sub>3</sub>)Rh(CO)<sub>2</sub> is nonluminescent at room temperature.<sup>6d,11b</sup> A comparison of the derived photophysical parameters illustrates that there are increases in k<sub>nr</sub> with factors between 1.8 and 2.4 for each of the three W(CO)<sub>5</sub>L complexes when the solvent is changed from methylcyclohexane to benzene (see Table 3). These ratios are very similar to the reduction in the φ<sub>CH</sub> values for (HBPz'<sub>3</sub>)Rh(CO)<sub>2</sub> on replacing *n*-pentane by benzene, where the factors are 1.9 at 458 nm and 2.5 at 366 nm (see Table 2). Thus, while we recognize that the decay rate constants are much lower for W(CO)<sub>5</sub>L than for (HBPz'<sub>3</sub>)Rh(CO)<sub>2</sub>, it appears that the effect of changing solvent on the nonradiative relaxation processes of the excited states is analogous.

The photochemistry of (HBPz'<sub>3</sub>)Rh(CO)<sub>2</sub> was also studied in mixed alkane/aromatic hydrocarbon solvents at 293 K. On 366-nm photolysis of the parent dicarbonyl complex in equimolar 4.9 M/4.9 M and 11.1 M/0.1 M *n*-pentane/benzene mixtures only the (HBPz'<sub>3</sub>)Rh(CO)(C<sub>6</sub>H<sub>5</sub>)H photoproduct was identified in the FTIR spectrum, indicating effective photochemical conversion of the pentyl derivative to the phenyl complex. Moreover, addition of benzene (1 volume) to a prior photochemically generated solution of the pentyl derivative, (HBPz'<sub>3</sub>)Rh(CO)(C<sub>5</sub>H<sub>11</sub>)H, in *n*-pentane (3 volumes) resulted in conversion in the dark, within 2–3 min, to the (HBPz'<sub>3</sub>)Rh(CO)(C<sub>6</sub>H<sub>5</sub>)H product again. These results further illustrate that the alkyl derivative is subject to thermal decomposition and in the presence of an aromatic solvent it forms the more thermodynamically stable aryl hydride complex (see eqs 10 and 11). This



process also appears to take place photochemically with 366-nm excitation enhancing the rate of conversion of the pentyl hydride species to the phenyl hydride product. Similar observa-

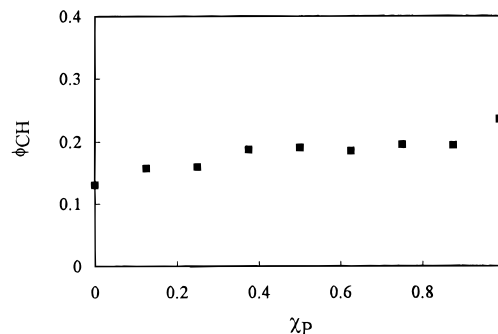


**Figure 4.** Plot of photochemical quantum efficiency (φ<sub>CH</sub>) at 366 nm for (HBPz'<sub>3</sub>)Rh(CO)<sub>2</sub> vs mole fraction of *n*-pentane (χ<sub>P</sub>) in *n*-pentane/benzene solutions.

tions were also made in *n*-hexane/toluene mixtures, resulting in (HBPz'<sub>3</sub>)Rh(CO)(C<sub>7</sub>H<sub>7</sub>)H exclusively as the final product.

Quantitative measurements of the C–H activation photochemistry of (HBPz'<sub>3</sub>)Rh(CO)<sub>2</sub> have been determined in several mixed *n*-pentane/benzene solutions. The results are shown in Figure 4 where the φ<sub>CH</sub> data at 366 nm can be observed to exhibit a dependence with the mole fraction (χ<sub>P</sub>) of *n*-pentane in various *n*-pentane/benzene solutions. This behavior is consistent with the above photophysical rationale linking the variations in φ<sub>CH</sub> with differences in the hydrocarbon nonradiative relaxation rates, as in the solution mixtures the k<sub>nr</sub> parameters can be expected to be intermediate between those of the pure solvents. Interestingly, these mixed solvent results exhibit a significant reduction in φ<sub>CH</sub> at high χ<sub>P</sub> values (e.g. φ<sub>CH</sub> = 0.24 for 11.1 M/0.1 M *n*-pentane/benzene) followed by a much more gradual lowering of φ<sub>CH</sub> in the χ<sub>P</sub> range of 0.1–0.9. This observation further supports the conclusion that the higher φ<sub>CH</sub> values in alkanes (see Table 2) are not a result of a kinetic preference for alkanes of the monocarbonyl primary photoproduct responsible for C–H activation. If there was a kinetic preference for alkanes in the mechanism then the magnitude of the φ<sub>CH</sub> values in the mixed *n*-pentane/benzene solutions ought to be closer to the higher number (*n*-pentane, φ<sub>CH</sub> = 0.32) rather than actually being closer to the lower number (benzene, φ<sub>CH</sub> = 0.13). Instead, the sharp lowering of φ<sub>CH</sub> on addition of a small amount of benzene suggests that there is selective solvation of the chromophore and that the effective concentration of benzene in the first solvation shell is higher than in the bulk solvent.

In summary, the quantum efficiencies for C–H bond activation in the different hydrocarbon solvents are influenced predominantly by the primary photophysical parameters and, specifically, the solvent effects on the rate of nonradiative relaxation from the upper LF excited state. The effectiveness of the light-induced intermolecular C–H bond activation process for (HBPz'<sub>3</sub>)Rh(CO)<sub>2</sub> in room-temperature solution is, therefore, ultimately determined by the efficiency of the dissociative route from the excited state leading to the primary photoproduct for any particular substrate and excitation wavelength. On this basis, it can now be understood why the φ<sub>CH</sub> data for (HBPz'<sub>3</sub>)-

Rh(CO)<sub>2</sub> in the aromatic solutions are lower than those for it in the alkanes, despite the fact that it is the aryl hydrido complexes which are the more thermodynamically stable photoproducts. Solvation effects on the photochemistry of other C–H-activating systems may also be influential and are currently being investigated.

**Acknowledgment.** We gratefully acknowledge the Division of Chemical Sciences, Office of Basic Energy Sciences, Office

of Energy Research, U. S. Department of Energy, for support of this work (Grant DE-FG02-89ER14039) and the Ministry of Education of the Republic of Indonesia for a doctoral fellowship to A.A.P. We also thank Professor W. A. G. Graham (University of Alberta) for initially supplying a sample of the title compound.

IC960479P